2014 IEEE International Conference on Robotics & Automation (ICRA)
Hong Kong Convention and Exhibition Center
May 31 - June 7, 2014. Hong Kong, China

Energy savings of a 2-DOF manipulator with redundant actuation

Giuk Lee, Donghun Lee, Jayil Jeong, and Jongwon Kim

Abstract*— This paper covers the energy-saving features of a robotics system by redundant actuation. By installing more actuators than the degrees of freedom, the actuating torques can be distributed. This distribution can reduce the overall energy loss, which reduces the overall energy consumption. An experiment was conducted with a 2-DOF general manipulator and redundant actuated manipulator; these were made to follow a typical welding pathway used in an automotive factory. The results showed that the redundant manipulator saved up to 38% electrical energy for actuation compared to the general manipulator.

I. Introduction

High-efficiency robotic systems can be achieved by reducing energy loss. When a robotic system is in operation, it requires electrical energy for input. This input energy is not only used for output energy but also consumed owing to energy loss. Therefore, reducing energy loss can improve the efficiency of a system.

Various studies have examined reducing energy loss. The previous researches were usually focused on trajectory planning; they attempted to optimize trajectories by measuring the performance in terms of effort and energy. Halevi et al. researched an optimal trajectory for minimum energy control of machine tool [1]. Field et al. researched an iterative dynamic programming for the optimal trajectory generation of robotic manipulator [2]. Bobrow et al. researched an optimal robot motions for physical criteria [3]. Moreover, there have been previous researches using gravity compensation devices such as counter weights and counter springs [4-7].

In this study, a new energy-saving feature is presented that the energy loss of robot manipulator can be reduced by redundant actuation. Redundant actuation can distribute the required torque for actuation, and the required current is proportional to torque. Because the energy loss is mainly proportional to the square of the current, this distribution of torque reduces the energy loss. Moreover, this suggested method can be applied with other methods counter balances and gravity compensation springs. To the best of our knowledge, no previous work has covered on this saving energy by redundant actuation.

This work was supported by the research program of Kookmin University in Korea, the IGPT Project (N0000005) of the Ministry of Knowledge Economy in Korea, and a National Research Foundation (NRF) grant funded by the Korean government (MEST) (No. 2012-0000348).

Giuk Lee, and Jongwon Kim are with the School of Mechanical and Aerospace Engineering, Seoul National University, Seoul, Korea (e-mail: gulee@rodel.snu.ac.kr; jongkim@snu.ac.kr).

Donghun Lee is with the Department of Mechanical Engineering, Soongsil University, Seoul, Korea (e-mail: dhlee04@ssu.ac.kr).

Jayil Jeong is with the School of Mechanical Engineering, Kookmin University, Seoul, Korea (corresponding author, tel:82-2-910-4419; fax: 82-2-910-4839; e-mail: jayjeong@kookmin.ac.kr)

The energy saving theory by redundant actuation is verified with simulations and experiments. A 2-DoF test manipulator which are modified from a base mechanism of general welding robots is used for the verification. A non-redundant mechanism and a redundantly actuated one are being operated with the same test pathway for verifying energy saving feature of redundant actuation. A simulation comparison about an energy consumption of those two manipulators is presented. Moreover, experimental results measuring electrical energy that the test manipulators consume is also depicted.

This paper is organized as follows. The energy-saving theory of redundant actuation is presented in Section 2. A dynamic and power consumption of a 2-DOF test manipulator is presented in Section 3. In Section 4, the simulation results about saving energy by redundant actuation are presented. The experimental verification with a test pathway is depicted in Section 5. Finally, concluding remarks follow in Section 6.

II. Concept

The input energy for actuating a robotic system is not only used for output work but also consumed as energy loss. There are many reasons for energy loss, but the main factor is coil loss in the motor. This loss is dissipated as heat in the motor and is proportional to the square of the current.

Fig.1 shows the basic concept of reducing energy loss by adding more motors. In the figure, the actuators are holding a 10 kg weight box as stop state. By adding more actuation, the required force in Fig.1(a) is distributed as shown in Fig.1(b).

In general, the required motor current is proportional to the

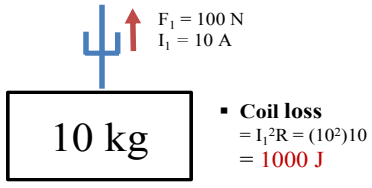

(a) Energy loss in generally actuated system

※ R(Coil resistance) = 10 Ω
Gravity acceleration = 10 m/s²

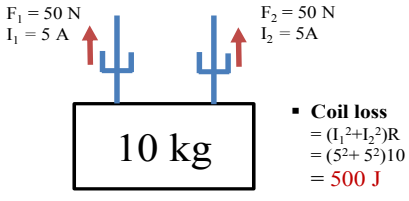

(b) Energy loss in redundantly actuated system

Figure 1. Reduction in energy loss by adding more actuation: energy loss in general and redundantly actuated systems

required torque. This means that distributing the force also distributes the required motor current. This feature can reduce the total energy loss because each motor coil loss is proportional to each square of the required current. In this concept, minimizing the sum of square forces can reduce the energy loss. Therefore, minimizing the sum of the square forces is the main objective function to reduce the energy loss.

This energy reduction concept can be applied even more efficient to robot manipulator systems. In Fig.2, a 2-DOF manipulator are holding 10 kg weight box as a stop state. By adding more motors, a 2-DOF general manipulator can be extended into a redundantly actuated manipulator as shown in Fig.2(b). This redundant manipulator can distribute the overall required torque of the general manipulator. Optimal distribution of the torques can minimize the sum of the square of actuation torques and reduce the energy loss over 50%.

III. Model

A. Dynamics model

A 2-DOF test manipulator based on a conventional manipulator IRB1410 by ABB is used for verification tests. Fig.3(a) shows a schematic diagram of the general manipulator. The main link (l_4) is connected to two linkage structures: (l_1, l_2) and (l_3). Two actuators were installed: B_1 and B_2.

As shown in Fig.3(b), the 2-DOF test manipulator was modified into a redundant manipulator. An additional linkage structure (l_5, l_6) and one motor B_3 were added. The dimension of this linkage structure is selected by referring to origin linkage structures, and will be optimized in future work.

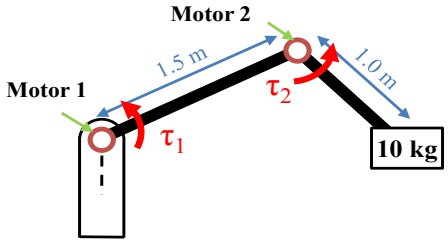

- $\tau_1 = 200$ Nm, $\tau_2 = 70$ Nm
- $\sum \tau^2 = 44{,}900$

(a) Sum of square torques in 2-DOF general manipulator

※ Gravity acceleration = 10 m/s ^{2}

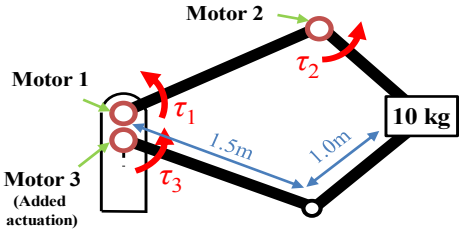

- $\tau_1 = 101.2$ Nm, $\tau_2 = 1.4$ Nm, $\tau_3 = 100.5$ Nm
- $\sum \tau^2 = 20{,}344$

(b) Sum of square torques in 2-DOF redundant manipulator

Figure 2. Application of energy loss reduction concept to robotics system: sum of square torques in 2-DOF general and redundant manipulators

As a result, the redundant manipulator comprises a main link (l_4) and three connecting linkage structures: (l_1, l_2), (l_3), and (l_5, l_6). This mechanism is still 2-DOF but is operated by three actuators: B_1, B_2, and B_3. Table I presents details on the lengths and weights of the linkages of the redundant manipulator.

The equations of motion for the proposed 2-DOF test manipulator in Fig.3 can be derived from the constraint equation, which represents the geometric constraint of the mechanism during its operation. The constraint equation can be expressed as follows:

$$\begin{bmatrix} g_1 \\ g_2 \\ g_3 \end{bmatrix} = \begin{bmatrix} \left\| {}^{B}\mathbf{P}_1(q_{r1}) - {}^{B}\mathbf{P}_2(q_{r2}) \right\| - \overline{J_1 J_2} \\ \left\| {}^{B}\mathbf{P}_2(q_{r2}) - {}^{B}\mathbf{P}_3(q_{r3}) \right\| - \overline{J_2 J_3} \\ \left\| {}^{B}\mathbf{P}_3(q_{r3}) - {}^{B}\mathbf{P}_1(q_{r1}) \right\| - \overline{J_3 J_1} \end{bmatrix} = \begin{bmatrix} 0 \\ 0 \\ 0 \end{bmatrix} \quad (1)$$

where ${}^{B}\mathbf{P}_i(q_{ri})$ denotes a position vector of joint J_i with respect to the base coordinate {B}. Position $\mathbf{P}_i$ depends on the angular value of q_{ri}, which is the angle command value of actuator B_i.

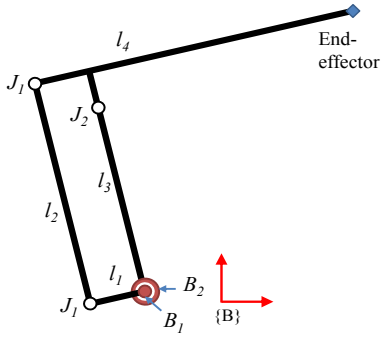

(a) Schematic diagram of 2-DOF general test manipulator

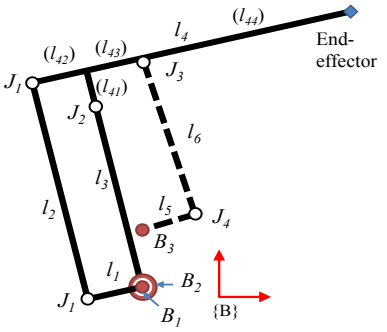

(b) Schematic diagram of 2-DOF redundant test manipulator

Figure 3. Schematic diagram of 2-DOF general and redundant manipulator.

TABLE I Specifications of 2-DOF redundant manipulator

Part name	Material	Length (mm)	Weight (kg)	Moment of Inertia (kg·m^2)
l_1	SM45C	230	3.7	0.07
l_2	A6061	960	3.7	1.21
l_3	SM45C	800	16	2.61
l_{41}	SM45C	160	21	6.99
l_{42}		230		
l_{43}		230		
l_{44}		850		
l_5	SM45C	230	3.7	0.07
l_6	A6061	710	2.8	0.50

Length $\overline{J_j J_k}$ represents the length between joints J_j and J_k.

The velocity relationships can be calculated using the constraint Jacobian relationship [8, 9]. This relationship can be obtained by the time derivative of the geometric constraint equation $g(\bullet)$. By collecting the actuating joints from the independent joints q_u and some of the dependent joints with actuators q_v, we can derive the relationship between the velocities of the independent and actuating joint angles as follows:

$$\dot{q}_r = VU\begin{bmatrix}\dot{q}_u \\ \dot{q}_v\end{bmatrix} = VU\begin{bmatrix}I_{2\times 2} \\ \Phi\end{bmatrix}\dot{q}_u = \Gamma\dot{q}_u \tag{2}$$

where q_u and q_r are the independent and actuating joint vectors, respectively. U is a transfer matrix from the independent and dependent joint vector to all of the joint vector. V is the selection matrix of the actuating joints from all of the joint vectors. Φ is a Jacobian mapping from the independent joints to the dependent joints. Γ is a Jacobian mapping from the independent joints to all of the actuating joints.

From (2), we can derive a relationship between torque vectors of the actuator in the general and redundant case as follows.

$$\tau_u = \Gamma^T\tau_r \tag{3}$$

where τ_u is a torque vector of the actuators in the general case and τ_r is a torque vector of the actuators in the redundant case. Because the number of active joints is greater than that of the independent joints in the case of the redundant manipulator, the actuation torque vector of redundant manipulator has non-unique solution.

The torques of the redundant actuation can be expressed by (4) for a minimum-norm torque distribution that minimizes the sum of square torques [10].

$$\tau_r = \Gamma(\Gamma^T\Gamma)^{-1}\tau_u \tag{4}$$

The dynamic equation of the redundant manipulator can finally be established as follows:

$$M\ddot{q}_u + C\dot{q}_u + N = \Gamma^T\tau_r \tag{5}.$$

B. Power consumption model

For simulation of the 2-DOF test manipulator, a power consumption model is analyzed. The power model consists of output power and power loss.

The output power means the power that actually performs an action in the motor. In case of positive output power, the motor uses input power for actuation. However, in case of negative output power value the power dissipates as heat since the motor usually cannot regenerate that power but lose the energy. Thus, the output power can be calculated as the sum of the product of torques and angular velocities of the actuating joints only if those product value has positive value, as shown in (6):

$$P_{mech} = \sum_{i=1}^{n}[\tau_i\dot{q}_i]^+ \tag{6}$$

where τ_i is the actuation torque and $\dot{q}_i$ is the angular velocity of the i-th actuating joint B_i. $[x]^+$ means that if x is larger than zero, [x] is x, otherwise [x] is zero.

The power loss of the test manipulator occurs in motors and amplifiers. The coil loss is the main contributor to the motor loss. This is heat loss caused by the flow of current [11]. The equation is given below:

$$P_{coil} = RI^2 \tag{7}$$

where R is the coil resistance and I is the motor current.

There are two types of power loss in the motor amplifier: conduction loss and switching loss [12, 13]. Each power loss occurs when current flows in an insulated gate bipolar mode transistor (IGBT) of the amplifier. The equation for conduction loss is as follows:

$$P_{cond} = c_{TA}I + d_{TA}I^2 \tag{8}$$

where c_{TA} and d_{TA} are constants for the conduction loss. The switching loss is given by the following equation:

$$P_{swit} = k_{IGBT}I \tag{9}$$

where k_{IGBT} is a constant for the switching loss.

Thus, the power consumption model is summation of the output power, coil loss, conduction loss and switching loss. Because the current is proportional to the torque, the power consumption model can be expressed as (10):

$$\begin{aligned}P_{cons} &= P_{mech} + P_{coil} + P_{cond} + P_{swit} \\ &= \sum_{i=1}^{n}([\tau_i\dot{q}_i]^+ + c_{1i}I_i + c_{2i}I_i^2) = \sum_{i=1}^{n}([\tau_i\dot{q}_i]^+ + k_{1i}|\tau_i| + k_{2i}\tau_i^2)\end{aligned} \tag{10}$$

To estimate the power model of the 2-DOF test manipulator, we measured the power consumption using the lookup table method. The power consumption was measured with power meter (CW121, YOKOGAWA) at the power source of actuation parts including the motors and amplifiers. Because the 2-DOF test manipulator has two types of actuation parts, each part was measured.

Because the output power can be calculated by (6), we only needed to measure the power loss. Therefore, the experiment was performed while keeping the motor in the stop position, which means that the output power was zero. We measured the consumption power according to the torque by changing the actuator load at 21 points.

Fig.4 shows the measurement results. The measurements were performed for each actuation part in the 3.0 kWh class (motor: SGMGH30A2A2C, amplifier: SGDH30AE by Yaskawa) and 4.4 kWh class (motor: SGMGH44A2A2C, amplifier: SGDH44AE by Yaskawa). The red line with triangles shows the 3.0 kWh estimation model. The blue line marked with circles shows the 4.4 kWh estimation model. Each marker shows a measurement point of the experiment.

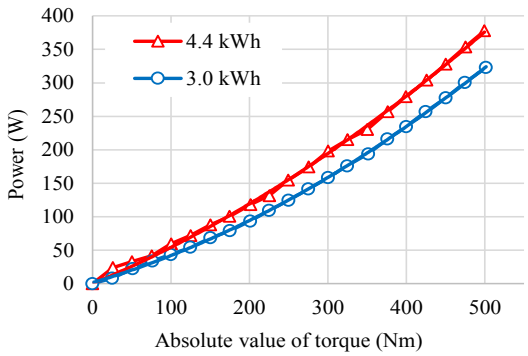

Figure 4. Measured power consumption of actuation part: 3.0 and 4.4 kWh classes

The constant of the power consumption model for the 2-DOF test manipulator in (10) was derived. k_{11} and k_{12} are 5.057×10^{-1}, and k_{13} is 3.666×10^{-1}. k_{21} and k_{22} are 4.708×10^{-4}, and k_{23} is 5.654×10^{-4}.

IV. Simulation

A. Test condition

The test pathway is shown in Fig.5, and it starts at position 1 and ends at position 7. This test pathway is used in the spot welding process at an automotive industry. The overall time of the test pathway is 78 seconds, and the maximum velocity of the end-effector was set to 290 mm/sec. The general and redundant manipulators were operated over the same test pathway with a 10 kg payload.

B. Distribution of actuation torques

The general manipulator had a unique solution of actuation torques during operation. However, the redundant manipulator can distribute the actuation torque of the electric motors, because it has non-unique solution. Therefore, we should determine how to distribute the actuation torques to reduce the power consumption.

The power consumption of actuators is mainly proportional to summation of the square values of each motor current. This means that the energy consumption can be reduced by minimizing the sum of the squares of each actuation torque. Therefore, the minimum-norm torque distribution is selected.

The objective of the minimum-norm torque distribution is to minimize the sum of squares of each redundant torque. The minimizing process was executed for the overall operation time. The performance index for the minimizing process of each time is shown in (11).

$$J(\tau) = \sum_{i=1}^{n} \tau_i^2 \tag{11}$$

where τ_i is the i-th joint actuation torque.

C. Simulation result

Fig.6 shows the actuation torques of general and redundant manipulators. The red solid line represents the actuation torque of B_1. The blue dashed line represents the actuation torque of B_2. The green alternated long and short dashed line

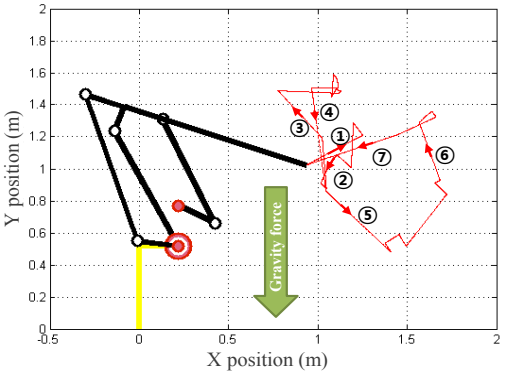

Figure 5. Test pathway of 2-DOF test manipulator.

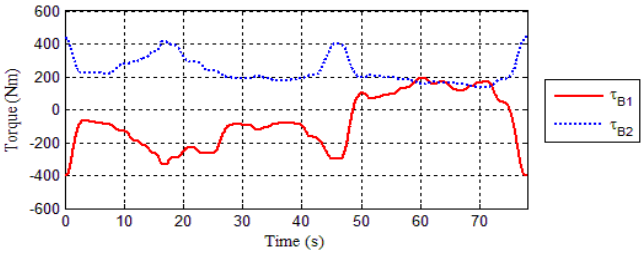

(a) Actuation torques of 2-DOF general manipulator

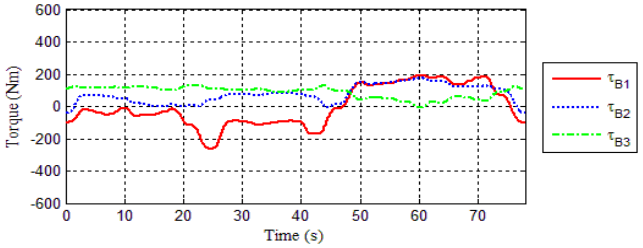

(b) Actuation torques of 2-DOF redundant manipulator

Figure 6. Simulation result: Actuation torque of 2-DOF general and redundant manipulators

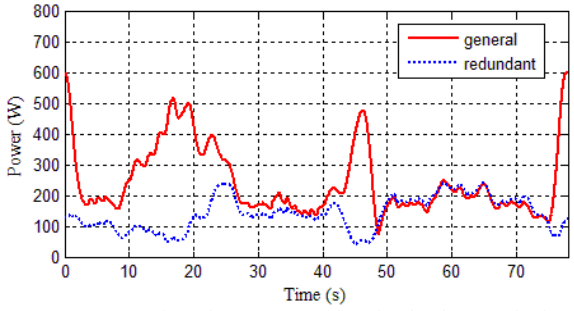

(a) Power consumption of 2-DOF general and redundant manipulators

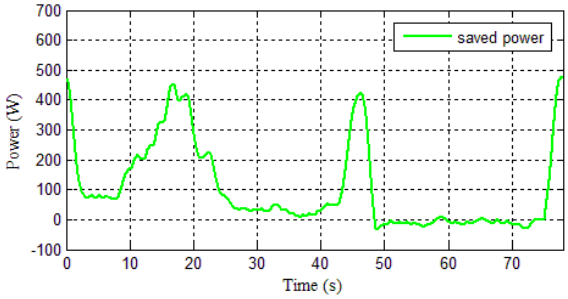

(b) Saved power by redundant manipulator

Figure 7. Simulation result: Consumed and saved power of 2-DOF general and redundant manipulators

represents the actuation torque of B_3. Fig.6(a) shows the actuation torques of general actuation. Fig.6(b) shows the actuation torques of redundant actuation with minimum-norm torque distribution.

Fig.7(a) depicts the power consumption of the general and redundant manipulators. The red solid line represents the power consumption of the general manipulator over the test pathway, where only two actuators at B_1 and B_2 were assumed to be in operation. The blue dashed line represents the power consumption of the redundant manipulator with minimum-norm distribution. The redundant manipulator used an additional linkage set and three actuators at B_1, B_2, and B_3

Fig.7(b) depicts the power saved by the redundant manipulator. The general manipulator was expected to consume 19,041 J of energy according to the simulation result. The redundant manipulator was expected to save 7983 J energy. The energy was calculated by integrating the power consumption during manipulation. The simulation results showed that the energy consumption by the redundant actuation was 41.9% less than that of the general actuation

V. Experiment

To verify the simulation results, experiments were carried out with the 2-DOF test manipulator depicted in Fig.8. The test manipulators were controlled by a Turbo-UMAC controller (DeltaTau). Fig.9 shows the comparison between simulation and experimental results of the actuation torques. The torques of actuators were measured from the electric source. The solid line represents experimental result, and the dashed line represents simulation result. The red line represents the actuation torque of B_1, the blue line represents the actuation torque of B_2, and the green line represents the actuation torque of B_3.

The total power consumption was measured with a power meter (CW121, YOKOGAWA) at the power source for all of the actuation parts. The power consumption included the power of all the motors and amplifiers.

The experiments were carried out for the general and redundant manipulators. Every experiment was performed for a test pathway with a 10 kg payload, where the maximum velocity of the end-effector was set to 290 mm/s. The redundant manipulator was operated with minimum-norm torque distribution control. In the minimum-norm torque distribution control, the actuators in the redundant manipulator can be controlled using independent control scheme for each actuator. That is, each actuator can be controlled using only the information from the corresponding encoder, rather than information from the encoders in the other actuators [10].

Fig.10 compares the simulation and experimental results for the power consumption of the general and redundant manipulators. The dashed line represents the simulation results, and the solid line represents the experimental results. The red line represents the energy consumption by general actuation, and the blue line represents the energy consumption by redundant actuation. The green line represents the energy saved by redundant actuation.

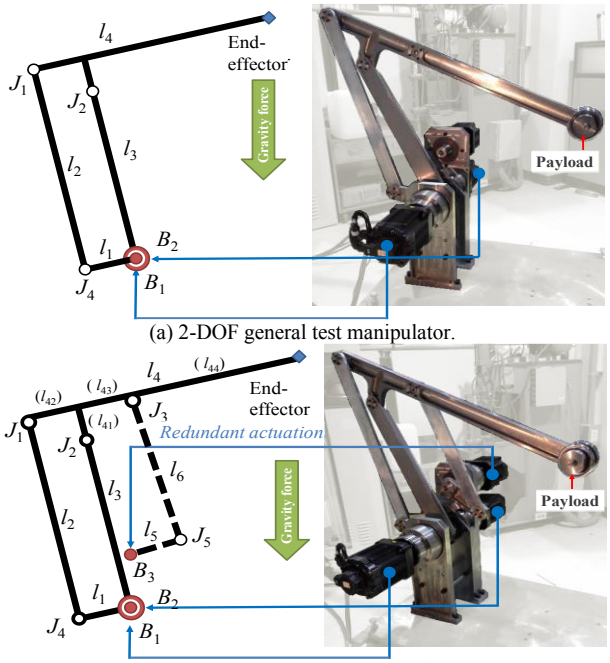

(a) 2-DOF general test manipulator.

(b) 2-DOF redundant test manipulator.

Figure 8. Two experimental setups for 2-DOF test manipulator with general and redundant actuation.

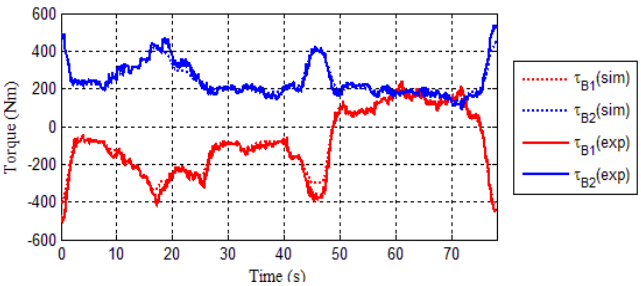

(a) Actuation torques of 2-DOF general manipulator

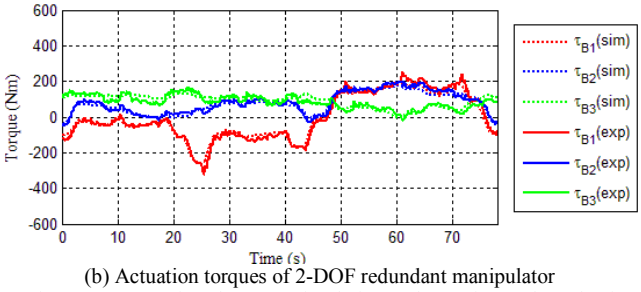

(b) Actuation torques of 2-DOF redundant manipulator

Figure 9. Comparison between simulation and experimental result of actuation torques

The experimental results were similar to the simulation results. The former showed that the energy consumed by the redundant manipulator was 38.0% less than that of the general manipulator. The saved energy was 7986 J. Table II compares the experiment and simulation results for the energy consumption in both cases.

VI. Conclusion

The energy-saving features of a redundantly actuated mechanism due to torque distribution are presented. Torque

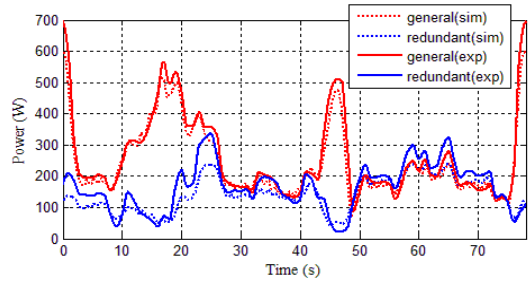

(a) Power consumption of general and redundant manipulators

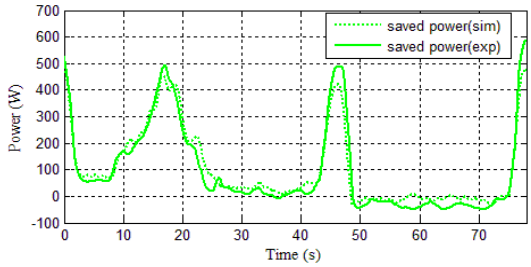

(b) Power saved by redundant manipulator

Figure 10. Comparison between simulation and experiment results of consumed and saved power

TABLE II SIMULATION AND EXPERIMENTAL RESULTS OF ENERGY CONSUMPTION

	General	Redundant	Rate of change
Simulation	19,041J	11,058 J	41.9 % saved
Experiment	21,022J	13,036 J	38.0 % saved

distribution can distribute the required current of the actuating motor, which can reduce the energy loss of the overall actuation system. A 2-DOF test manipulator was made to follow a welding test pathway in an experiment and operated using a minimum-norm torque distribution.

Both the simulated and experimental results showed that that the redundant manipulator reduced the energy consumption compared to the general manipulator. The experimental result showed that the redundant manipulator saved up to 38.0% of the energy along the test pathway. This result shows the novel advantage of the redundant mechanism from an energy perspective. This energy-saving feature is effective in robotics systems that are greatly affected by gravitational forces. As a future work, the workspace will be tested. Pathways will be analyzed to clarify the energy saving feature with respect to the workspace, and the workspace change for kinematic chains modified will be analyzed too.

REFERENCES

[1] Y. Halevi, E. Carpanzano, G. Montalbano and Y. Koren, "Minimum energy control of redundant actuation machine tools," in *Annals of CIRP*, vol. 60, no. 1, pp. 433-436, 2011.

[2] G. Field and Y. Stepanenko, "Iterative dynamic programming: an approach to minimum energy trajectory planning for robotic manipulators," in *IEEE International Conference on Robotics and Automation*, vol. 3, pp. 2755-2760, 1996.

[3] B. J. Martin and J. E. Bobrow, "Minimum-effort motions for open-chain manipulators with task-dependent end-effector constraints," in *The international journal of robotics research*, vol. 18, no. 2, pp. 213-224, 1999.

[4] J. E. Bobrow, B. Martin, G. Sohl, E. C. Wang, F. C. Park and J. Kim, "Optimal robot motions for physical criteria," in *Journal of Robotic systems*, vol. 18, no. 12, pp. 785-795, 2001.

[5] Y. Li and G. M. Bone, "Are Parallel Manipulators More Energy Efficient?," in *Proc. 2001 IEEE International Symposium on Computational Intelligence in Robotics and Automation*, pp. 41-46, 2001.

[6] M. Freese, S. P. N. Singh, E. F. Fukushima, S. Hirose, "Bias-Tolerant Terrain Following Method for a Field Deployed Manipulator", *in IEEE International Conference on Robotics and Automation*, pp. 175-180, 2006.

[7] S. K. Agrawal, A. Fattah, "Gravity-balancing of spatial robotic manipulators," *Mechanism and Machine Theory*, vol. 39, pp. 1331-1344, 2004.

[8] F. C. Park and J. W. Kim, "Singularity analysis of closed kinematic chain," in *ASME Journal of Mechanical Design*, vol. 121, no. 1, pp. 32-38, 1999.

[9] Y. Nakamura and M. Ghodoussi, "Dynamics computation of closed-link robot mechanisms with nonredundant and redundant actuators," in *IEEE Transactions on Robotics and Automation*, vol. 5, no. 3, pp. 294-302, 1989.

[10] H. Cheng, Y. K. Yiu and Z. Li, "Dynamics and control of redundantly actuated parallel manipulators," in *IEEE/ASME Transactions on Mechatronics*, vol. 8, no. 4, pp. 483-491, 2003.

[11] C. T. Raj, S. P. Srivastava and P. Agarwal, "Energy efficient control of three-phase induction motor-a review," *International Journal of Computer and Electrical Engineering*, vol. 1, no. 1, pp. 1793-8198, 2009.

[12] U. Drofenik and J. W. Kolar, "A general scheme for calculating switching-and conduction-losses of power semiconductors in numerical circuit simulations of power electronic systems," in *Proc. IPEC*, 2005.

[13] I. Kioskeridis and N. Margaris, "Loss minimization in induction motor adjustable-speed drives," *IEEE Transactions on Industrial Electronics*, vol. 43, no. 1, pp. 226-231, 1996.